

DISCRIMINATIVE GRAPHICAL MODEL FOR POROUS MEDIA IMAGE SYNTHESIS*

E. AHMADI¹, Z. AZIMIFAR^{2**}, P. FIEGUTH³ AND S. AYATOLLAHI⁴

^{1,2}School of Electrical & Computer Engineering, Shiraz University, Shiraz, I. R. of Iran
Email: azimifar@cse.shirazu.ac.ir

³Systems Design Engineering, University of Waterloo, Waterloo, Canada

⁴School of Petroleum & Chemical Engineering, Shiraz University, Shiraz, I. R. of Iran

Abstract– Imaging synthesis methods open a new door to help scientists for further study on porous materials. High resolution images are required to analyze the macroscopic properties of porous media. However, a few degenerated high resolution samples are available because of constraints, and low resolution measurements (such as MRI images) cannot fully describe the medium. Computer-aided approaches can help the science of porous media by generating many artificial high resolution samples using the information of available data. In this paper, a novel discriminative graphical framework is proposed which statistically models the synthesis problem. The probability distribution of high resolution image of a porous medium given a low resolution measurement is modeled by conditional random fields (CRF). A Monte Carlo approach is proposed to sample the constructed model and to generate high resolution samples. Moreover, a hierarchical CRF is proposed for gradual synthesis of high resolution porous media images. The success of the models is shown and compared through several experimental results.

Keywords– Porous media, image synthesis, graphical models, conditional random fields

1. INTRODUCTION

Scientific imaging is an exploding field, especially due to the proliferation of a wide range of imaging modalities and instruments. In particular, medical imaging and remote sensing are two such areas which have been extensively studied. However, there are other areas still awaiting further study, such as the science of porous media. Porous media is the science of porous materials such as cement, wood, cartilage, rock and soil [1], which have significant contributions in construction, medicine, environmental industries, and petroleum engineering.

To study and to analyze the macroscopic properties (porosity, permeability, conductivity and etc.) of porous materials, a large ensemble of high-resolution images is required [2]. Some examples of high-resolution microscopic images of porous media are shown in the first row of Fig. 5, where the black/white shading shows the two phases of pore and solid. Providing high resolution physical samples requires cutting, polishing, exposure to air and, consequently, a variety of influences and alterations to samples. On the other hand, the acquisition of 3D MRI images has no impact on the sample, but has limited spatial resolution, such that only large pores can be resolved. Therefore, image processing and computer vision methods can be very helpful to synthesize new high resolution images for further studying of porous materials [3]. In other words, the information of available high- and low resolution images can be fused to model the characteristics of porous medium and, then, sampling the constructed model provides us high resolution images with consistent properties of original images of the medium.

*Received by the editors November 17, 2013; Accepted November 15, 2014.

**Corresponding author

As a result of constraints (physics, time and expense), few high resolution samples are available. Moreover, multiple measured samples are typically not from a single scene, therefore, super-resolution and multi-resolution data fusion approaches may not be useful. However, porous media samples do have some sort of structure and randomness, for which statistical methods can be quite successful, therefore, we are interested to model the statistical characteristics of images of such media for the purpose of synthesis.

Almost all the primary works build the model just based on high resolution images. The model is sampled for the synthesis of new high resolution images. A number of statistical functions such as two-point correlation and chord length distribution are used as prior models [4]. The process is called prior sampling and does not use low resolution images. However, with respect to advanced 3D imaging tools, low resolution images also have complementary information which can be used for the description of porous medium. In the first attempt of fusing low resolution measurements with high resolution data, Okabe and Blunt [5] proposed a stochastic reconstruction method. In their method, large pore structure is resolved using low resolution tomographic images and small-scale ones are reconstructed using learned prior model independent of low resolution measurement. The first problem of this method is that the low resolution measurements are not explicitly coupled with prior model of high resolution images. The other limitation is that all the information provided by low resolution images cannot be fully exploited.

A more robust statistical method was proposed by Mohebi et al. [6], in which Gibbs random field (GRF) is used for prior modelling. The prior model is built as the fusion of chord length and histogram distributions from high resolution images. In an approach named posterior sampling, the reconstructing sample based on the prior model is constrained by low resolution measurements. Therefore, to some extent, the prior model is coupled with measurement model in the process of posterior sampling. Although the method has great success in the reconstruction task, some delicate points can be considered for further investigation. The first point is that the method models the probability distribution of high resolution images of porous medium and makes the synthesizing sample close to measurements during the sampling phase. However, modelling the probability distribution of high resolution images given the low resolution measurements is more consistent with the nature of our image synthesis problem. Moreover, in this approach, constraining the reconstructing sample means reduction of the distance between the measurement obtained from the reconstructing image and the true available measurement. However, the true underlying function (forward problem function) of extracting low resolution image from the high resolution one is not known. The last issue to be addressed is that the contribution of the prior model and low resolution measurement in reconstruction process is not fully coupled in [6] which is explained more later in this paper.

We proposed a novel framework of image synthesis very naively in our preliminary work [7]. A discriminative graphical model, conditional random field (CRF), is used to model the probability distribution of high resolution images given the low resolution measurements. The CRF model was firstly proposed by Lafferty et al. [8] for segmenting and labeling sequencing data. This discriminative graphical model directly models the conditional distribution instead of modelling the joint probability distribution of generative methods such as Markov random field (MRF) [9]. The success and superiority of CRF have been proved in many computer vision applications [10-13]. CRF is used to model the distribution of high resolution images, since low resolution ones make the synthesizing model more consistent with the nature of the problem. Moreover, the contributions of prior and measurement models are fully integrated. Besides all of these points, the function to convert the high resolution sample to low resolution measurement is no longer required and the relation between low- and high resolution images is implicitly modelled in CRF.

The first contribution of this paper is that our previous method is presented in a more detailed and revised manner. Hierarchical approaches are introduced in many computer vision applications [14-16]. Due to scale to scale synthesis of high resolution images, we propose a hierarchical conditional random

field (HCRF) to model the synthesis task as our second main contribution. The third novelty in this work is designing informative feature functions to describe porous medium in both our CRF and HCRF models. The fourth and last contribution is proposing novel sampling algorithms to sample from the learned models.

The rest of the paper is organized as follows. The statistical formulations of the porous media image synthesis task in the previous works compared to our proposed models are explained in Section 2. Section 3 presents our proposed CRF-based approach for image synthesis, and HCRF model is introduced in Section 4. Section 5 includes the experimental results and discussions. Finally, the paper is concluded in Section 6.

2. STATISTICAL FORMULATION

Due to existing constraints, synthesis of high resolution porous media images using computer-aided methods attracts a great deal of interest. Among these methods, statistical approaches are the focus of this paper. Early works model the probability distribution function of high resolution image $P(H)$ of a porous medium and the artificial samples are generated using the sampling algorithms. However, as mentioned in Section 1, the low resolution measurements can play a significant role in describing porous medium because of their supplementary information to high resolution images.

Okabe and Blunt [5] model the distribution $P(H)$, however, the distribution $P(H_{unres.}|H_{res.})$ is sampled in the sampling phase. In fact, $H_{res.}$ represents the portion of the reconstructing image which is fully resolved by the available low resolution measurements. Therefore, the sampler infers the unresolved part $H_{unres.}$ of image H . It is obvious that the information of low resolution is not completely used for reconstruction in this method.

The probability distribution $P(H)$ is also modelled by Mohebi et al. [6] using GRF as:

$$P(H) = \frac{1}{Z} \exp\left(\frac{-E(H)}{T}\right) \quad (1)$$

where, Z and T represent the normalization factor and the temperature, respectively. Function $E(H)$ is the energy function which characterizes the porous medium in this framework. To take advantage of low resolution measurement M in the synthesis phase, the authors constrain the probability distribution in sampling process such that:

$$P(H|M) = \frac{1}{Z(M)} \exp\left(\frac{-E(H|M)}{T}\right) \quad (2)$$

where, the energy function is substituted by:

$$E(H|M) = E(H) + \alpha ||f(H) - M|| \quad (3)$$

where, $f(\cdot)$ indicates a preassumed forward model by which the measurement is extracted from the reconstructing image H . As a result, the measurement M does not play any role in modelling phase but forces the sampling image to be consistent with itself. Moreover, the contribution of prior and measurement energies are separated and are controlled by the hand-tuning parameter α . Eq. (2) can be rewritten as:

$$\begin{aligned} P(H|M) &\approx \frac{1}{Z_1} \exp\left(\frac{-E(H)}{T}\right) \times \frac{1}{Z_2} \exp\left(\frac{-\alpha ||f(H) - M||}{T}\right) \\ &= P(H) \times P(M|H) \end{aligned} \quad (4)$$

where, $P(H)$ and $P(M|H)$ represent prior and likelihood models, respectively. Equation (4) shows the separation of prior and measurement effects in the synthesis problem. Moreover, it is shown that the model can be categorized as generative model, although it can be inferred from the equivalence of GRF and MRF models [17].

In many machine learning and computer vision problems, the superiority of discriminative models are discussed and proved in comparison to generative models [18]. In this paper, conditional random field (CRF) is used as a discriminative graphical model for the modelling of our image synthesis task. Our CRF directly models the distribution $P(H|M)$ instead of separating it to prior and likelihood models. The measurement M also contributes in construction of the probability distribution function rather than just playing a role in sampling phase. As discussed in the next section, it is not required to know the forward model $f(\cdot)$ and the information of available low- and high resolution images is fully coupled in our modelling framework.

3. PROPOSED CRF-BASED FRAMEWORK

The goal of this paper is to propose a novel framework which is consistent with the nature of our image synthesis problem. In porous media image synthesis problem which is the focus of this paper, a few high resolution images and a number of low resolution measurements of a porous medium are available. The objective is to learn a model which characterizes the medium and can be used for synthesis of new high resolution samples. For the purpose of simplicity, all the high and low resolution images are supposed to be 2D and only one image from each set is available for training. While the model is being learnt, each time the sampler is run, the goal is to infer a high resolution image H^* given a low resolution measurement M :

$$H^* = \overline{\operatorname{argmax}}_H P(H|M) \quad (5)$$

It is proposed that we model the distribution $P(H|M)$ by conditional random field (CRF). Sites of H are random variables corresponding to image pixels which compose a random field. Each site (pixel) of H is considered to be a vertex of a graph G in which neighbouring pixels are connected to each other. The neighbours of a site (i, j) are determined due to a predefined neighbourhood system. Considering vertices V and edges E , graph $G = (V, E)$ conditioned on M is called CRF and the probability distribution P is determined as a product of factors defined on G :

$$P(H|M) = \frac{1}{Z(M)} \prod_{c \in C} \prod_{c' \in c} \psi_{c'}(H_{c'}, M) \quad (6)$$

where, each factor c' is called a clique which contains a set of nodes, every two of which are mutual neighbours. A clique template c is a representative of similar cliques of G and the set C includes all clique templates defined based on the neighbourhood system. Parameter $Z(M)$ is the normalization constant and function $\psi_{c'}(\cdot)$ is the potential function associated with clique c' , which is defined as:

$$Z(M) = \sum_{H'} \prod_{c \in C} \prod_{c' \in c} \psi_{c'}(H_{c'}, M) \quad (7)$$

$$\psi_{c'}(H_{c'}, M) = \exp\left(\sum_{n=1}^{N(c')} \sum_{h_{c'}} w_{n, h_{c'}}^{c'} f_n^{c'}(H_{c'}, M) I(H_{c'} = h_{c'})\right) \quad (8)$$

where, H' represents any arbitrary configuration of high resolution random field and $f_n^{c'}(H_{c'}, M)$ is the n -th function of $N(c')$ feature functions defined on clique c' of H and measurement M . Parameter $w_{n, h_{c'}}^{c'}$ is the weight of $f_n^{c'}(H_{c'}, M)$ for each configuration $h_{c'}$ of $H_{c'}$ and I represents the indicator function.

Some primary assumptions are made to cope with the high complexity of general CRF. This paper (similar to almost all CRF applications) selects first order neighbourhood system for the CRF model such that sites $\{(i, j-1), (i-1, j), (i, j+1), (i+1, j)\}$ are the neighbours of site (i, j) . As a result, three clique templates exist in the model. The proposed CRF-based image synthesis model and the first order neighbourhood system and its corresponding clique templates are shown in Fig. 1.

Supposing random field H to be isotropic (stationary with respect to rotation of cliques), the vertical and horizontal double-site cliques will be identical. Therefore, we are left with only single-site and double-site clique templates and we call them *node* and *edge* cliques, respectively. Moreover, it is

supposed that the random field H is homogeneous (stationary with respect to shifting of cliques), then the same feature functions are defined for the same cliques and their corresponding weight parameters are shared between them (known as parameter tying). By substituting (8) in (6) and considering the mentioned assumptions, the probability distribution of CRF can be rewritten as:

$$P(H|M) = \frac{1}{Z(M)} \exp(\sum_i E^{node}(H_i, M) + \sum_i \sum_{j \in Ne(i)} E^{edge}(H_i, H_j, M)) \quad (9)$$

where, i and j are the indices of i -th and j -th sites and $Ne(i)$ includes the neighbours of site i . Parameters E^{node} and E^{edge} are called the energy functions associated with *node* and *edge* cliques, respectively.

$$E^{node}(H_i, M) = \sum_{n_1=1}^{N(node)} \sum_{h_i \in S} w_{n_1, h_i}^{node} f_{n_1}^{node}(H_i, M) I(H_i = h_i) \quad (10)$$

$$E^{edge}(H_i, H_j, M) = \sum_{n_2=1}^{N(edge)} \sum_{h_i, h_j \in S} w_{n_2, h_i, h_j}^{edge} f_{n_2}^{edge}(H_i, H_j, M) I(H_i = h_i, H_j = h_j) \quad (11)$$

where, in this paper, $S = \{0,1\}$ (corresponding to pore or solid state of each pixel) is the set of states from which each site can receive its value.

The CRF-based porous media image synthesis problem is modelled by Eqs. (9)-(11). However, to fully characterize the porous medium, the *node* and the *edge* feature functions should be defined. Moreover, the weight parameters of the model are tuned using training data.

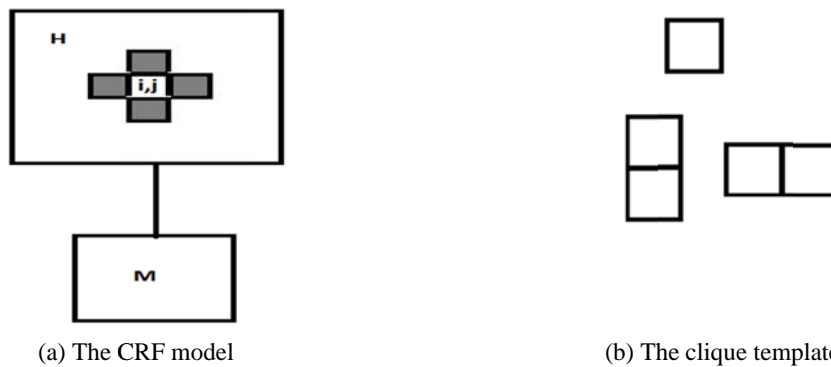


Fig 1. The proposed CRF-based image synthesis Framework: the CRF model and the first order neighbourhood system is shown in (a). Three clique templates corresponding to the neighbourhood system is depicted in (b)

a) Parameter estimation and inference

Let us assume we have K identically independently distributed (i.i.d) training data $\{(H^{(k)}, M^{(k)}): k = 1, 2, \dots, K\}$, the parameters $w = \{w_{n,s}^{node}, w_{n,s_1,s_2}^{edge}\}$ can be estimated using maximum likelihood estimation (MLE) method. The MLE method finds the parameters w^* such that the log-likelihood function ℓ of training pairs is maximized:

$$\begin{aligned} \ell(w) &= \log(\prod_{k=1}^K P(H^{(k)}, M^{(k)})) \\ &= \sum_{k=1}^K \left(\sum_i E^{node}(H_i^{(k)}, M^{(k)}) + \sum_i \sum_{j \in Ne(i)} E^{edge}(H_i^{(k)}, H_j^{(k)}, M^{(k)}) - \log(Z(M^{(k)})) \right) \quad (12) \end{aligned}$$

Since function $\ell(w)$ is concave [19], this optimization problem can be solved using iterative gradient ascent method.

Computing the probability of an arbitrary configuration of H given a measurement M or finding the best H^* that maximizes (5) is called inference. For the CRF model which has a cyclic graph, loopy belief propagation (LBP) [20] is a common method of inference. It is a sum-product message passing algorithm that calculates the marginal distribution.

b) Feature functions for CRF-based model

In literature, statistical functions such as chordlength and histogram-based distributions are used to characterize porous media images [1]. Inspired by these features, we design novel features for our proposed CRF model. Suppose that one 2D high resolution image H and one 2D low resolution image M are available for training. The pixel values of H belong to $\{0,1\}$ and the intensities of M are gray values distributed over the interval $[0,1]$.

The first feature of each node i is set to $f_1^{node}(H_i, M) = 1$ as bias feature. We call the second and the third features fuzzy [21] horizontal chordlength and fuzzy vertical chordlength features which are defined as:

$$f_2^{node}(H_i, M) = \sum_{r=pr(i)-r_1}^{pr(i)+r_2} \mu_{solid}(M_r) \quad (13)$$

$$f_3^{node}(H_i, M) = \sum_{c=pr(i)-c_1}^{pr(i)+c_2} \mu_{solid}(M_c) \quad (14)$$

where, $pr(i)$ indexes a site in M which is the parent of i -th site of H . Parameter $\mu_{solid}(M_r)$ is the degree of intensity value M_r in a fuzzy set named *solid*. In other words, $\mu_{solid}(M_r)$ determines to what degree the pixel M_r is a solid (white) pixel. Therefore, f_2^{node} finds a horizontal chord in M with length of $(r_1 + r_2 + 1)$ corresponding to H_i where all pixels of the chord have greater membership degree in either *solid* or *pore* fuzzy sets and returns the summation of the degrees. Low/High feature value indicates the existence of a *pore/solid* (black/white) horizontal chord around M_r , respectively. The *pore* and *solid* fuzzy membership functions are two Gaussian functions of means equal to zero and one which is shown in Fig. 2. The function f_3^{node} is analogous to f_2^{node} for the vertical configuration around site $pr(i)$ of M .

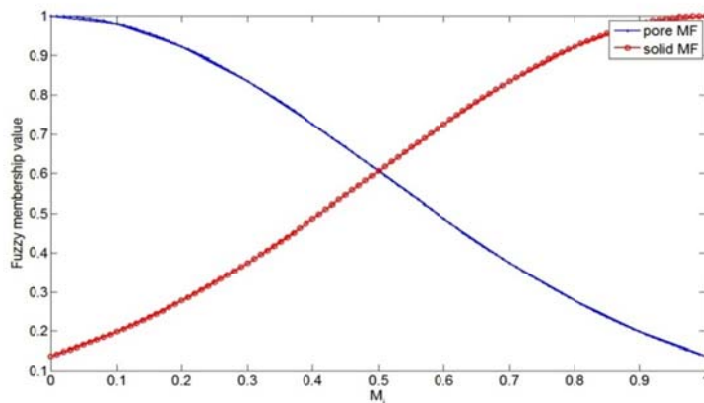


Fig. 2. The fuzzy membership function of being pore or solid pixel

The fourth proposed feature is the summation of fuzzy membership values of a 3×3 window centred on site $pr(i)$ within image M :

$$f_4^{node}(H_i, M) = \sum_{j \in win(pr(i))} \mu_{solid}(M_j) \quad (15)$$

As it is obvious, the concept of fuzziness is used for designing the features to extract the inexact information of measurement field M . All the features associated with node H_i characterize the i -th node of the high resolution image H based on given measurement M . However, the decision about a site as being a *pore* or *solid* pixel is not made only based on node features. The power and impact of graphical models, especially CRF, is that they use the information of neighbouring pixels. In other words, it is expected that the neighbouring pixels have the same behaviour. This is modelled by edge features in CRF model. Four edge features are also designed in our model such that the first one is $f_1^{edge}(H_i, H_j, M) = 1$ similar to node features. The other three features are defined as:

$$f_n^{edge}(H_i, H_j, M) = \frac{1}{1 + |f_n^{node}(H_i, M) - f_n^{node}(H_j, M)|} \quad (16)$$

where the i -th and j -th sites with close features have edge features near one and dissimilar neighbour sites tend to have near zero edge features. Therefore, edge features model the interaction between neighbouring pixels in H . A porous medium is fully characterized by both node and edge features.

c) Proposed sampling

While the CRF model $P(H|M)$ is defined and its parameters are learnt, high resolution images can be sampled given every test low resolution measurement M . A Gibbs sampler along with simulated annealing procedure can sample the probability distribution [7, 22]. Sampling is started with a random configuration of H at a high temperature T_0 . The Gibbs sampler samples the value of H_i for each node i due to its marginal distribution:

$$P(H_i|M) = \frac{1}{Z_i(M)} \exp\left(\frac{E^{node}(H_i, M) + \sum_{j \in Ne(i)} E^{edge}(H_i, H_j, M)}{T}\right) \quad (17)$$

The procedure repeats until a stopping criterion is reached. The exponential $T_{iter} = T_0 \times b^{iter-1}$ cooling schedule is used for the sampling method.

Experiments show that edge energies E^{edge} dominate the node energies and this causes over-smoothing in the sampling process of the Gibbs annealing sampler (GAS). Therefore, smaller structures cannot be well resolved during the annealing. We propose a novel sampling method to deal with the problem. The sampling process is divided into two phases. In the first phase, the edge energy is ignored and a high resolution image is sampled by the Gibbs annealing sampler starting from T_0 and ending in T_{min} . By fixing the temperature at T_{min} , the sampling is continued with both energy terms (node and edge energies) for a number of times in the second phase. We call the first and second phases the formation and smoothing stages, respectively. Experimental results have shown the success of our proposed two-stage Gibbs annealing sampler (TSGAS) compared with the common GAS method.

4. PROPOSED HCRF-BASED FRAMEWORK

Hierarchical methods have drawn attention in many computer vision works [14-16]. In this section, we propose a hierarchical conditional random field for our porous media image synthesis problem. Without loss of generality, it is supposed that H and M are of size $2^n \times 2^n$ and $2^m \times 2^m$, respectively. The parameters n and m , where $m < n$, are considered as the scales of images H and M , respectively. In our proposed hierarchical framework, the information is gradually passed scale to scale from the coarse scale m to the fine scale n . We propose that from scale $m + 1$ to scale n , samples R^s are synthesized based on R^{s-1} and M , where R^i is the reconstructed estimate of the high resolution image at scale i . A hierarchical CRF (HCRF) is proposed in order to construct a model characterizing the porous medium in this framework. The conditional distribution of R^s given R^{s-1} and M is defined as

$$P(R^s | R^{s-1}, M) = \frac{1}{Z(R^{s-1}, M)} \exp(\sum_i E^{node}(R_i^s, R^{s-1}, M) + \sum_i \sum_{j \in Ne(i)} E^{edge}(R_i^s, R_j^s, R^{s-1}, M)) \quad (18)$$

where, the node energy function E^{node} and the edge energy function E^{edge} can be rewritten as:

$$E^{node}(R_i^s, R^{s-1}, M) = \sum_{n_1=1}^{N(node)} \sum_{h_i \in S} w_{n_1, h_i}^{node} f_{n_1}^{node}(R_i^s, R^{s-1}, M) I(R_i^s = h_i) \quad (19)$$

$$E^{edge}(R_i^s, R_j^s, R^{s-1}, M) = \sum_{n_2=1}^{N(edge)} \sum_{h_i, h_j \in S} w_{n_2, h_i, h_j}^{edge} f_{n_2}^{edge}(R_i^s, R_j^s, R^{s-1}, M) I(R_i^s = h_i, R_j^s = h_j) \quad (20)$$

The graphical representation of the proposed HCRF image synthesis model is shown in Fig. 3. The main difference is that the features of HCRF model use the information of the coarser-scale high resolution reconstructed image R^{s-1} .

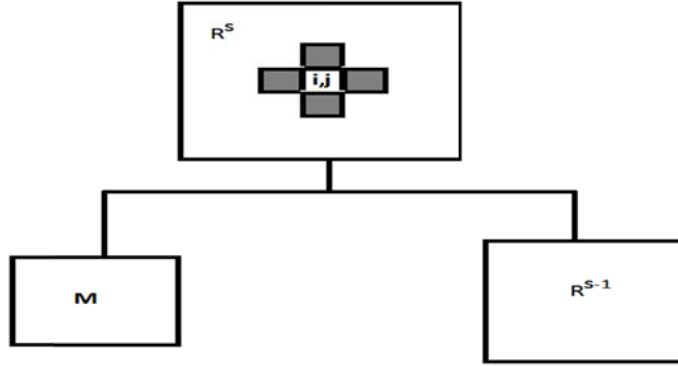


Fig. 3. The graphical scheme of our proposed HCRF image synthesis model

a) Feature functions in HCRF model

In our proposed HCRF model, our four proposed CRF node features are revised such that the information of coarser reconstructed image R^{s-1} confirms or denies the states of pixels in R^s . The first node feature is the bias feature as was introduced in Section 3.2 and the other three feature functions are defined as:

$$f_2^{node}(R_i^s, R^{s-1}, M) = \sum_{r=pr(i)-r_1}^{pr(i)+r_2} (R_r^{s-1} + 1) \times \mu_{solid}(M_r) \quad (21)$$

$$f_3^{node}(R_i^s, R^{s-1}, M) = \sum_{c=pr(i)-c_1}^{pr(i)+c_2} (R_c^{s-1} + 1) \times \mu_{solid}(M_c) \quad (22)$$

$$f_4^{node}(R_i^s, R^{s-1}, M) = \sum_{j \in win(pr(i))} (R_j^{s-1} + 1) \times \mu_{solid}(M_j) \quad (23)$$

It is obvious that the pixel values of the reconstructed image R^{s-1} boost or diminish the original features. In other words, the information of the reconstructed coarser scale image R^{s-1} affects the features so that pixels of finer scale image R^s can more discriminatively be chosen to be pore or solid ones.

The edge features are the same as the features defined in CRF model. The HCRF model is trained as CRF model and then it is sampled to generate new high resolution images of the porous medium.

b) Proposed hierarchical sampling

While the parameters of the HCRF image synthesis model are tuned using training data, high resolution images can be synthesized given a low resolution sample. It is proposed that the sampling is started at scale m and a high resolution sample of scale $m + 1$ is generated given the low resolution image M and a heuristic high resolution estimate R^m . The process generates a high resolution sample R^s given the synthesized sample R^{s-1} and the low resolution measurement M at scale s . A high resolution image at scale n is the desired generated sample. The sampling method used in each scale can be any of those explained in Section 3. Using the proposed HCRF framework, the information of low resolution measurement is propagated gradually scale to scale and results in a more robust high resolution sample. The schematic process of our proposed hierarchical sampling framework is depicted in Fig. 4.

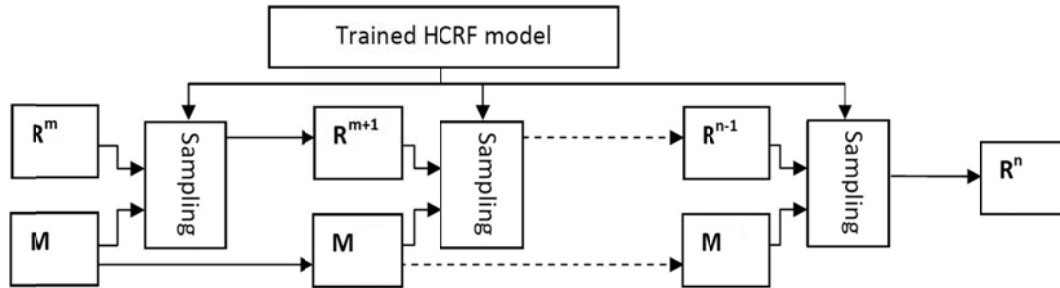


Fig. 4. The diagram of our proposed hierarchical sampling approach

5. EXPERIMENTAL RESULTS

To evaluate the proposed algorithms, we design different experiments on seven porous media images with various structures and one toy case (case 8). The original samples are shown in the first row of Fig. 5. The second row of the figure contains the low resolution measurements corresponding to each sample, where the parameter dsR indicates the down sampling rate. The low resolution images are generated artificially such that every $dsR \times dsR$ block of original image is averaged as the measurement. Our proposed methods are compared with the method proposed in [6] and our previous work [7]. It is worthwhile to say that the superiority of the method of [6] compared to the one [5] is shown in [6]. The summation of chordlength and histogram distributions is used as the energy functions in (3). The ising-directed features are also implemented for the method of [7].

Our proposed CRF and HCRF models are trained using the pair of high and low resolution images for each case shown in Fig. 5. The proposed GAS and TSGAS sampling methods are run to sample the trained models given their corresponding low resolution measurements. At first glance, the visual inspection of the results in Fig. 6 shows the superiority of our proposed method compared with the methods of [6] and [7]. Moreover, it is visually evident (especially in case 3) that our TSGAS sampling method can much better synthesize the structures and does not have oversmoothing artifacts with respect to GAS method.

For more illustrative evaluation, the mean squared error (MSE) between the original and reconstructed images is used as a quantitative criterion. The MSE between an original image O and a reconstructed image R is computed as:

$$MSE(O, R) = \frac{1}{n} \sum_i (O_i - R_i)^2 \quad (24)$$

where, parameter n represents the number of sites of the images. Figure 7 compares the methods based on MSE criterion on all samples. The eight samples are reconstructed by the six methods with multiple low resolution measurements generated by different $dsR = [2, 4, 8, 16]$ (242 images). The last image (case 8) is a toy porous image with different pore structure and size.

The ascending curves of Fig. 7 indicates that lower resolution measurements have much less information and make reconstructed samples with higher errors. The method of [6] attempts to make the reconstructing high sample close to the low resolution measurement by constraining the sampling process. As the measurements with $dsR = 2$ have more information and are very close to high resolution images, the method of [6] can perform better in some cases. However, our proposed model is a more general method and samples the unified model of $P(H|M)$ in a more natural manner. The generalization of our method is more obvious as dsR increases. The superiority of our proposed algorithm with respect to that of [6] is obviously shown with the increase of dsR . Moreover, the TSGAS better performance can also be seen in these MSE curves. Our proposed hierarchical model also has comparable results. Moreover, the

reconstructed samples in each scale can be used as the initial state of the finer scale sampling process and it can help the faster convergence of our hierarchical approach. The gradual passing of information through the scale to scale sampling process results in more detailed high resolution samples.

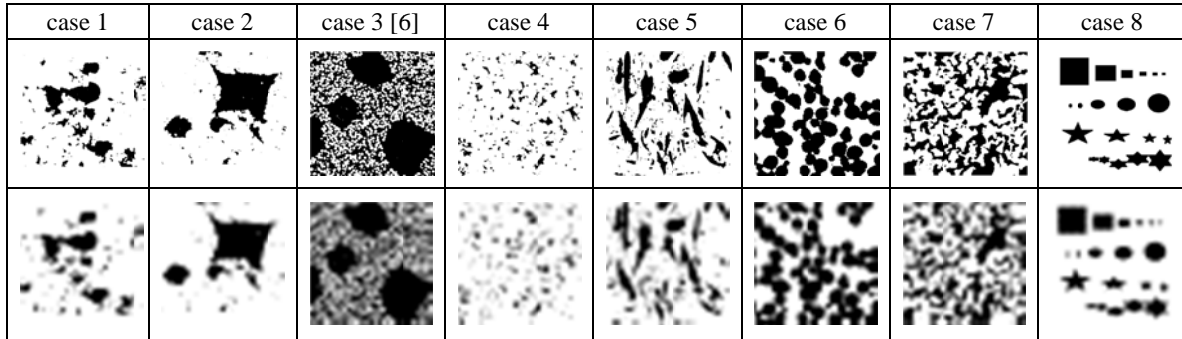


Fig. 5. The ground-truth images are shown in the first row. The second row contains generated artificial samples by downsampling ($dsR=16$). Case 8 is a toy image with different pore size and pore structure.

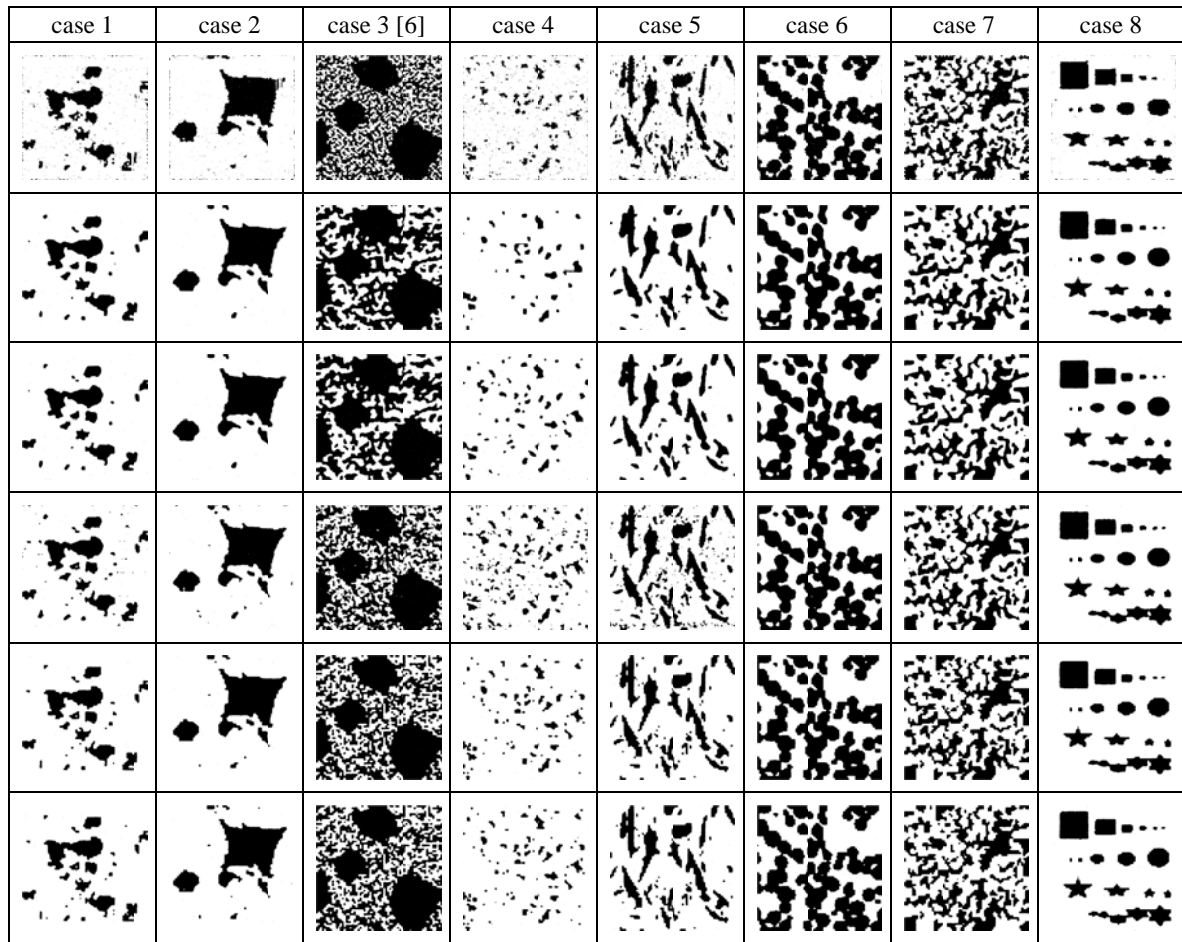


Fig. 6. The first and second rows are the samples reconstructed by [6] and [7], respectively. The other rows are the samples reconstructed by our proposed methods: CRF+GAS (row 3), CRF+TSGAS (row 4), HCRF+GAS (row 5) and HCRF + TSGAS (row 6)

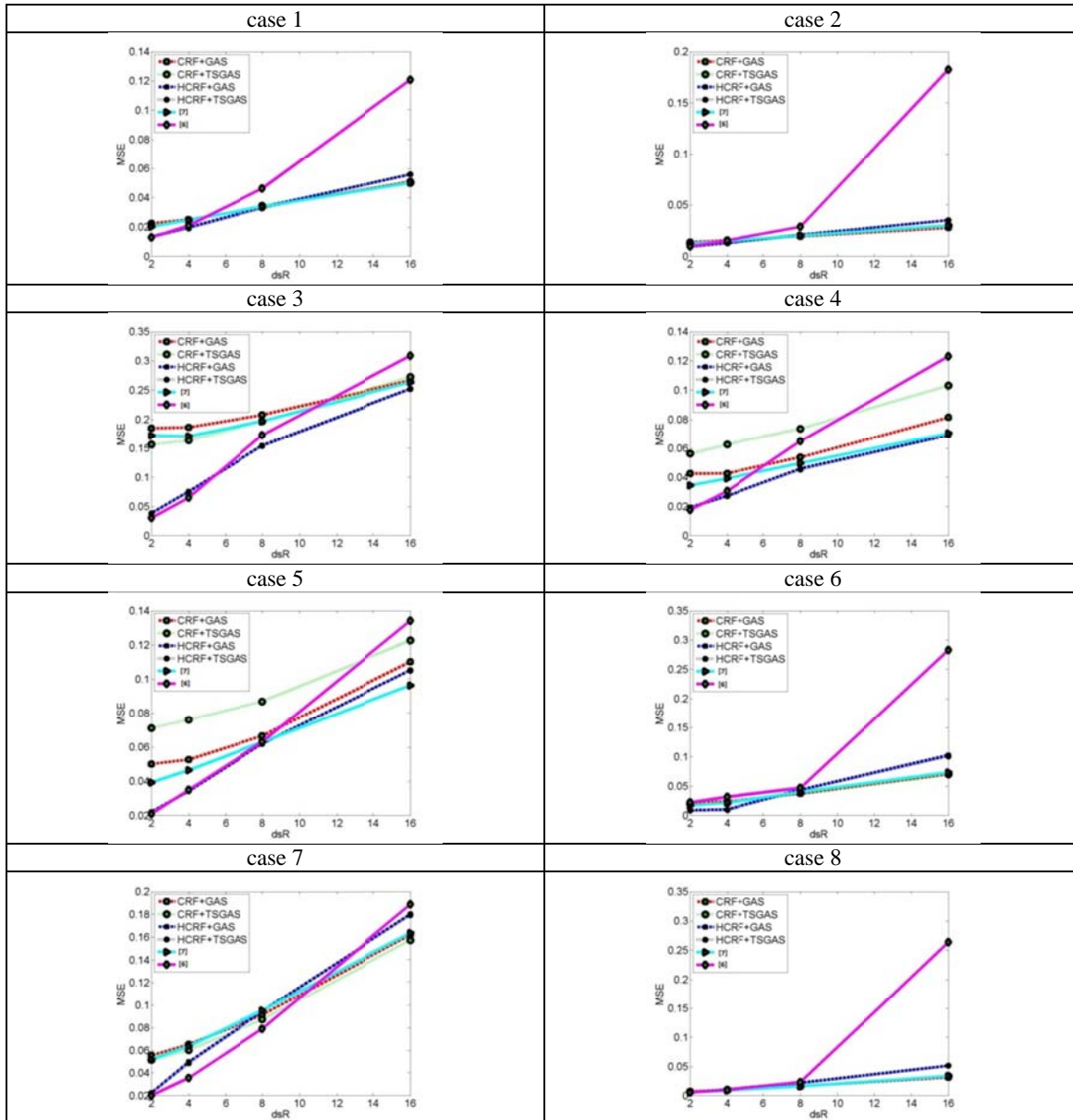


Fig. 7. The MSE between the original high resolution images and the reconstructed images using different methods. The sampling methods are applied on measurements of various downsampling rates

It should be noted that our CRF and HCRF models do not need the forward model (as the one used in [6] does) to use the information of low resolution measurements in sampling. Further, the function of forward problem is not commonly known in most vision problems and our independent synthesis of high resolution images is the most important advantage of the proposed framework.

Despite the theoretical superiority of our model (does not need to know the forward problem function and is more consistent with the nature of porous media image synthesis task), the results show the success of our previously published model [7] in comparison to the one of [6]. It indicates the capability of our first CRF model. The proposed CRF+GAS method of this paper is the same as our previous method [7] but with new designed features. The better results of CRF+GAS method in most of the cases in comparison to [7] show that more informative features are proposed in this paper. Through the results, it is shown that the proposed TSGAS sampling method also improved the GAS one. It can be concluded that

our CRF method is a more compatible model compared to the one of [6] for the image synthesis task. This method is also improved by designing new informative features and more successful sampling process. Although the proposed HCRF model has comparable results compared to others, it is itself a valuable framework because of its hierarchical approach.

6. CONCLUSIONS AND FUTURE WORK REMARKS

In this paper, the synthesis of high resolution porous media images given the low resolution measurements is modelled using CRF. The proposed discriminative framework is consistent with the nature of the problem and facilitates the information fusion of low and high resolution images for the synthesis task. Novel feature functions are designed to describe the porous medium characteristics and new sampling approach is introduced. Moreover, gradual synthesis process is introduced by proposing a novel hierarchical CRF model and hierarchical sampling. The visual and numerical inspections of results prove the superiority and success of our proposed framework compared to existing ones.

Designing more descriptive feature functions for our proposed models and generalization of the models for the synthesis of 3D images are our main future directions in this field.

REFERENCES

1. Adler, P. M. (1992). *Porous media, geometry and transports*. Butterworth-Heinemann series in chemical engineering, Butterworth-Heinemann.
2. Mohebi, A. & Fieguth, P. (2006). Posterior sampling of scientific images. *ICIAE*. pp. 339-350.
3. Kaestner, A., Lehmann, E. & Stampanoni, M. (2008). Imaging and image processing in porous media research. *Advances in Water Resources*, Vol. 31, pp. 1174-1187.
4. Torquato, S. (2002). *Random heterogeneous materials: microstructure and macroscopic properties*. Springer-Verlag.
5. Okabe, H. & Blunt, M. J. (2007). Pore space reconstruction of vuggy carbonates using microtomography and multiple-point statistics. *Water Resour Res*, Vol. 43.
6. Mohebi, A., Fieguth, P. & Ioannidis, M. A. (2009). Statistical fusion of two-scale images of porous media. *Advances in Water Resources*. pp.1567-1579.
7. Ahmadi, E., Azimifar, Z., Fieguth, P. & Ayatollahi, Sh. (2010). Image Synthesis using Conditional Random Fields. *International Conference on Image Processing (ICIP)*. IEEE, pp. 3997-4000.
8. Lafferty, J., McCallum, A. & Pereira, F. (2001). Conditional random fields: Probabilistic models for segmenting and labeling sequence data. *Proc. ICML*. pp. 282-289.
9. Li, S. Z. (2009). *Markov random field modeling in image analysis*. Springer.
10. Klinger, R. & Tomanek, K. (2007). *Classical probabilistic models and conditional random fields*. Dortmund University of Technology.
11. Sutton, C. & McCallum, A. (2007). *An introduction to conditional random fields for relational learning*. Introduction to Statistical Relational Learning, MIT Press.
12. Ahmadi, E., Garmsirian, F. & Azimifar, Z. (2012). A discriminative fusion framework for skin detection. *Artificial Intelligence and Signal Processing (AISP), 2012 16th CSI International Symposium on*, IEEE. pp. 542-545.
13. Fosler-Lussier, E., He, Y., Jyothi, P. & Prabhavalkar, R. (2013). Conditional Random Fields in Speech, Audio and Language Processing. *Proceedings of the IEEE*, Vol. 105, pp. 1054-1075.
14. He, X., Zemel, R.S. & Carreira-Perpinán, M.A. (2004). Multiscale conditional random fields for image labeling.
15. Fieguth, P. Hierarchical posterior sampling for images and random fields. (2003). *ICIP*. pp. 821-824.

16. Reynolds, J. & Murphy, K. (2007). Figure-ground segmentation using a hierarchical conditional random field. *Computer and Robot Vision. CRV'07. Fourth Canadian Conference on*, IEEE. pp. 175–182.
17. Hammersley, J. M. & Clifford, P. (1971). Markov fields on finite graphs and lattices.
18. Bishop, C.M. (2006). Pattern Recognition and Machine Learning. *Information Science and Statistics*.
19. Nowozin, S. & Lampert, C. H. (2011). Structured learning and prediction in computer vision. *Foundations and Trends in Computer Graphics and Vision*, Vol. 6, pp. 185-365.
20. Vishwanathan, S., Schraudolph, N., Schmidt M. & Murphy, K. (2006). Accelerated training of conditional random fields with stochastic meta-descent. ICML.
21. Farahbod, F. & Eftekhari M. (2013). A new clustering-based approach for modelling fuzzy rule-based classification systems. *Iranian Journal of Science and Technology, Transaction of Electrical Engineering*, Vol. 37, pp. 67-77.
22. Geman, S. & Geman, D. (1984). Stochastic relaxation, gibbs distribution and the bayesian restoration of images. *IEEE Trans. PAMI*, pp. 721-741.